Multiple Sensor Indoor Mapping Using a Mobile Robot

Timothy E. Lee / leete@stanford.edu / CS229 Final Project

Introduction

Mapping – the ability for a robot to observe and build a representation of its environment – is a critical task for mobile robots. Indeed, mapping is a necessary component of autonomous navigation, in addition to perception and localization. Mapping is achieved by measuring the environment with sensors, such as laser, sonar, or visual-based techniques, and using probabilistic models to estimate the state of the environment. For indoor mobile robots, mapping can be used to build the indoor environment boundary (e.g., building walls). This study will investigate how multiple sensors can be used in concert to generate a map of the indoor environment using a mobile robot. Understanding the improvement of multiple sensor mapping over single sensor mapping may prove valuable in the design of mobile robots and autonomy routines, as tradeoffs may exist between any improvement in mapping accuracy and the decrease in weight, useful payload capability, and increase in computational resources for installing and utilizing the additional sensors.

Goal and Scope

The goal and scope of this study is to generate a map that estimates an indoor environment given robot sensor data, and determine whether a fusion of sensor data can improve the accuracy of the map over using one sensor.

Data

The selected dataset to investigate multiple sensor indoor mapping is the dataset collected from a Pioneer 2-DX mobile research robot exploring the first floor of Gates Computer Science Building at Stanford University for approximately 30 minutes. The data are available online in the Robotics Data Set Repository (Radish), courtesy of B. Gerkey [1]. The robot was equipped with a variety of sensors to record laser, sonar, and odometry data:

- Laser range data were collected using a SICK Laser Measurement Sensor (LMS200) that was attached to the robot. Laser readings were collected at approximately 60 Hz. Each laser reading contains 181 measurements, corresponding to 1 degree intervals sweeping from one side of the robot to the other. In total, 118,312 laser readings are available in the dataset.
- Sonar range data were collected from the sonar array installed on the robot. The sonar array is composed of 16 individual sensors spaced entirely around the robot. 20,724 sonar readings were collected at a sampling frequency of approximately 10 Hz.
- Odometry (or position) data were collected from the robot at approximately 10 Hz. 20,724 odometry readings are available in the dataset. Each reading provides the robot pose (x-position, y-position, and heading), translational velocity, and rotational velocity.

It should be noted that the dataset lacks a quantitative ground truth map, which precludes certain analyses. A map of the indoor environment is provided, but it has no resolution, distances, landmarks, or color scale. Thus, extracting position and probability estimates from the ground truth map is not feasible. Therefore, mapping the indoor environment will be considered to be a supervised learning problem only in the sense that a *qualitative* assessment of the generated map's accuracy is possible (i.e., how similar does it appear to the ground truth map).

Models

Learning the map of an indoor environment can be accomplished by generating an occupancy grid map $m = \{\boldsymbol{m}_i\}$ [2]. The occupancy grid is a discretized representation of the indoor environment, where each cell of the grid carries the probability of that grid cell being free (not occupied). Probabilistically, each cell of the occupancy grid is modeled as a binary random variable, with value of 1 for free and value of 0 for occupied. The likelihood that a particular cell $\boldsymbol{m}_i$ of the occupancy grid is free based on the robot pose $x_{1:t}$ and evidence (i.e., sensor data) $z_{1:t}$ acquired until the present time t is

$$p(\boldsymbol{m}_i|z_{1:t}, x_{1:t})$$

The construction for the entire occupancy grid can thus be expressed as a product of marginals given pose and evidence:

$$p(m|z_{1:t}, x_{1:t}) = \prod_i p(\boldsymbol{m}_i|z_{1:t}, x_{1:t})$$

The real-time algorithm to construct the occupancy grid map is accomplished by processing the data chronologically, and the cells within the perceptual field of the robot are updated whenever a sensor reading occurs [2]. The robot pose is updated in parallel using the odometry data. The perceptual field provides evidence that a certain grid cell is occupied based on the range measurement (i.e., distance), and provides non-occupied evidence for cells located in between the occupied cell and the robot. A separate map for each sensor is maintained. At the conclusion of the algorithm, the maps generated from each sensor are combined to form one map, completing the multiple sensor indoor mapping routine. For this study, all algorithms were implemented using MATLAB.

Regarding the parameters of the model, the prior of occupancy is assumed to be 0.5, meaning equal probability initially that the cell is either occupied or free. The weight of the sensor evidence also plays a key role in the model. Without available quantitative ground truth, the probability of receiving a sensor pulse from a particular cell given the cell is occupied is assumed to be 0.55, and the probability of no sensor pulse from a particular cell (within the perceptual field) given the cell is free also assumed to be 0.55. These probabilities are low to account for pedestrians and other dynamic considerations of the indoor environment that would cause spurious data; however, there is sufficient volume of sensor data to estimate the occupancy map for either sensor.

Results and Discussions

Single Sensor Mapping

The first attempt at generating the indoor map for the entire dataset using the laser sensor revealed uncorrected odometry errors in the dataset, as shown in Figure 1. The source of these errors is caused by how the robot determines its position. The Pioneer 2-DX robot integrates the measured wheel velocities into position estimates (using bearing data provided by a compass) in a process known as dead reckoning [3]. However, errors within the measurement of wheel state and bearing also become integrated and therefore grow without bound. Hence, the use of position in the occupancy grid algorithm must be adjusted in some way to account for these odometry errors. While a variety of techniques have been proposed to estimate and remove this error, they require information beyond what is available in the dataset (e.g., using accelerometer data from a gyroscope [4], or by calibrating the robot by moving in a pre-defined square pattern [5]).

Because the odometry errors manifest through integration, these integrated errors will remain small for small time segments. Thus, to provide an indoor map in the presence of odometry errors, the occupancy map for a limited portion of the overall dataset is instead examined. This limited portion is the first 3 minutes of the indoor tour, and the qualitative ground truth for this portion is shown in Figure 2. The number of binary random variables representing the occupancy of the map for this reduced portion of the discretized indoor environment is approximately 50,000.

Figure 3 shows the single sensor occupancy grids generated for the cases of using the laser in isolation and the sonar in isolation. Unsurprisingly, the laser sensor provides well-defined boundaries and open floors, which is expected due to the high sampling rate and excellent resolution of the laser range measurements. Some odometry error is present, but otherwise, the map is similar to the qualitative ground truth map. For the occupancy grid generated from sonar data, the overall probabilities are lower in open hallways. However, the sonar occupancy grid sufficiently predicts the boundaries of this environment, so this occupancy grid generally agrees with the qualitative ground truth (disregarding odometry errors).

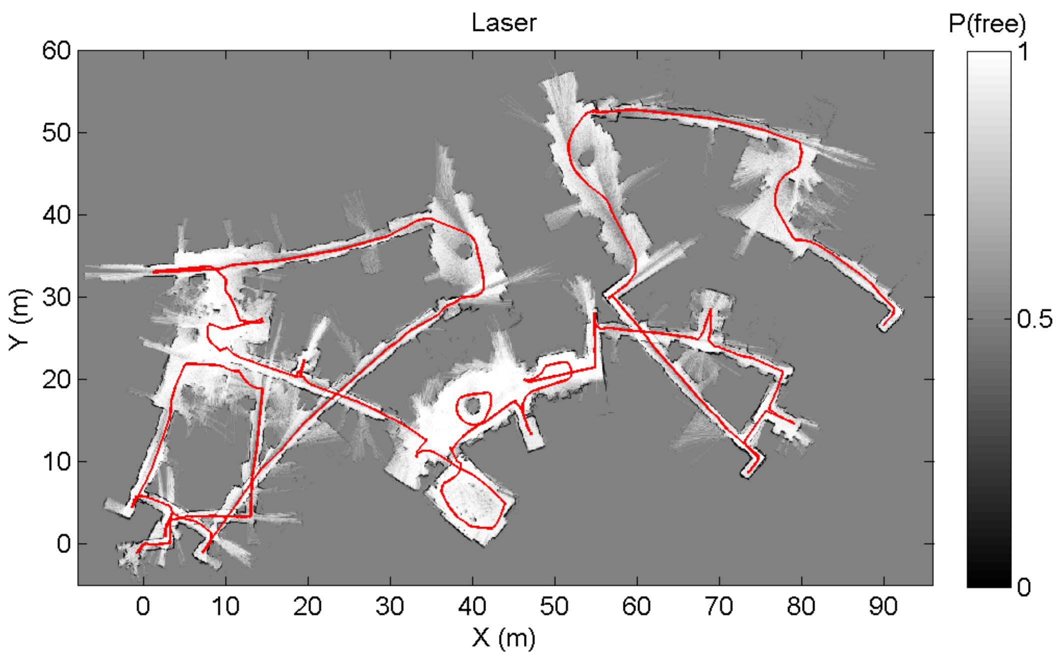

Figure 1: Occupancy grid map for the entire dataset as determined from laser measurements. The overlap is caused by latent odometry errors in the dataset. The robot trajectory is superimposed.

Multiple Sensor Mapping

Having generated separate maps for both the laser and the sonar sensors, the next step for fusing the sensor information is the selection of fusion algorithm. One particular algorithm is provided that, for each grid cell, keeps the minimum value over the maps generated by k sensors [2]:

$$\boldsymbol{Pessimistic\ Fusion}: p(\boldsymbol{m}_i) = \min_k p\left(\boldsymbol{m}_i^k\right)$$

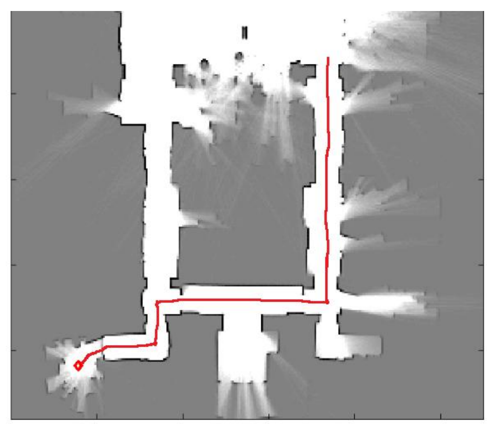

Figure 2: The qualitative ground truth for the occupancy grid mapping problem. The approximate robot trajectory is superimposed.

This algorithm is described as pessimistic because, for each grid cell, the sensor with the lower probability of that cell being free (higher probability of being occupied) is selected. In other words, the fusion algorithm trades less mapping of potential areas of further exportation (such as open doors and corridors that are better captured by the laser) for higher probabilities of detecting boundaries. This is evident in Figure 4 when comparing the multiple sensor occupancy grid to the map generated by the laser sensor in Figure 3. Figure 4 also indicates the sensor source for each grid cell; it suggests that the laser is providing better probability estimate for walls and a higher probability estimate of free grid cells in hallways.

The results from the pessimistic sensor fusion suggest that the laser is superior to the sonar for classifying grid cells into either free or occupied states, and therefore, for mapping this environment. This is likely due to the higher sampling rate of the laser sensor as compared to the sonar sensor. However, because their underlying measurement mechanisms are different, some object types in the indoor environment may be better suited for detection by one sensor, rather than the other. For example, the sonar sensor has readings entirely around the robot (and thus can perceive objects behind the robot), whereas the laser can only perceive objects in the direction of the robot heading.

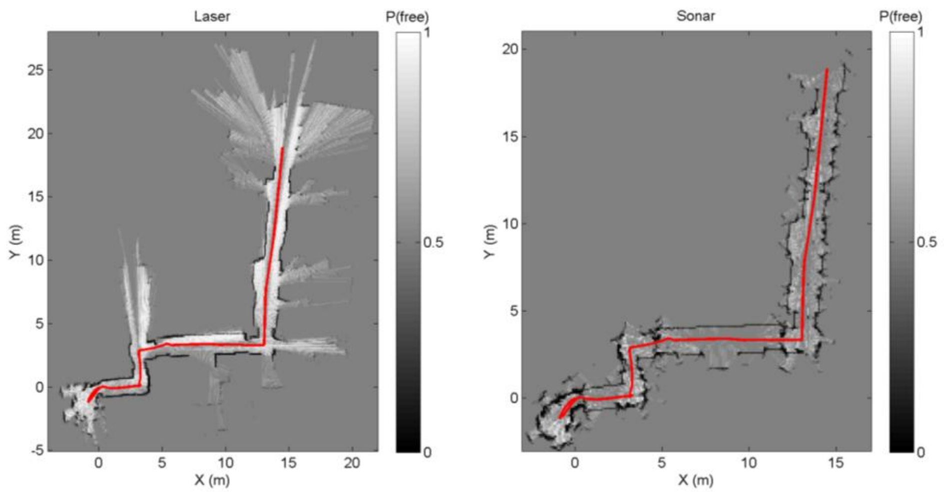

Figure 3: Occupancy grid maps for using the laser alone (left) and the sonar alone (right).

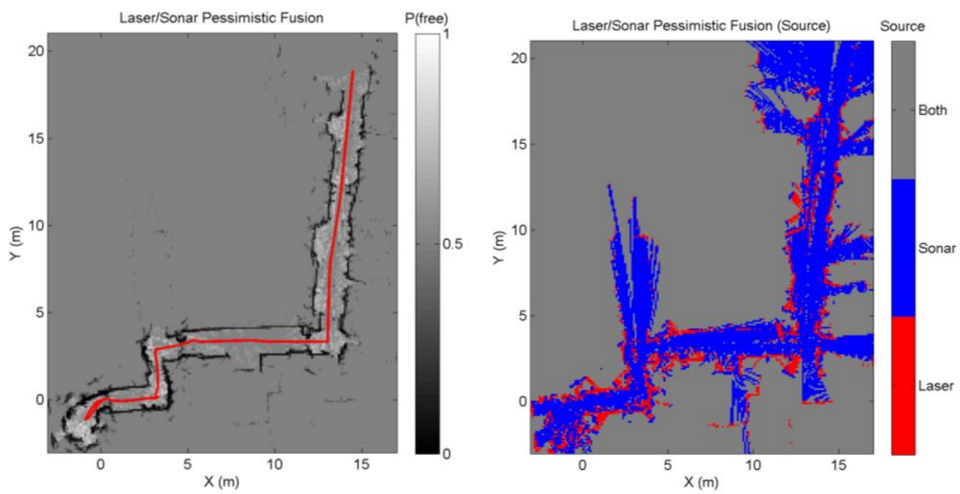

Figure 4: Occupancy grid map generated from multiple sensors using a pessimistic fusion algorithm (left). The sensor source for each cell is also shown (right).

Therefore, it is desirable to choose the sensor with the highest confidence in the classification of grid cells (as either occupied or free). To this end, a fusion algorithm is proposed that uses the sensor with the most confident classification:

$$\boldsymbol{MinMax\ Fusion}: p(\boldsymbol{m}_i) = \begin{cases} \max\limits_{k} p(\boldsymbol{m}_i^k) & \text{if avg}\left(p(\boldsymbol{m}_i^k)\right) > 0.5 \\ \min\limits_{k} p(\boldsymbol{m}_i^k) & \text{if avg}\left(p(\boldsymbol{m}_i^k)\right) < 0.5 \\ 0.5 & \text{otherwise} \end{cases}$$

The calculation of average probability over k sensors is necessary to understand if the sensors are generally indicating a free cell (and thus use the sensor with highest probability) or an occupied cell (and thus use the sensor with lowest probability of being free, i.e., highest probability of being occupied). The occupancy grid for the MinMax sensor fusion is shown in Figure 5. It is evident that this fusion permits the use of laser readings in states where it outperforms the sonar (e.g., through long hallways and open doors), but also relies on the sonar for better occupied cell detection of boundaries in the room at location (-1, -1). The difference between the laser occupancy grid and MinMax fusion occupancy grid is subtle, but the MinMax fusion grid appears to offer a better estimate of the indoor environment than the single sensor grid. This is achievable because sonar measurements are used when the sonar grid estimates are superior to the laser grid estimates.

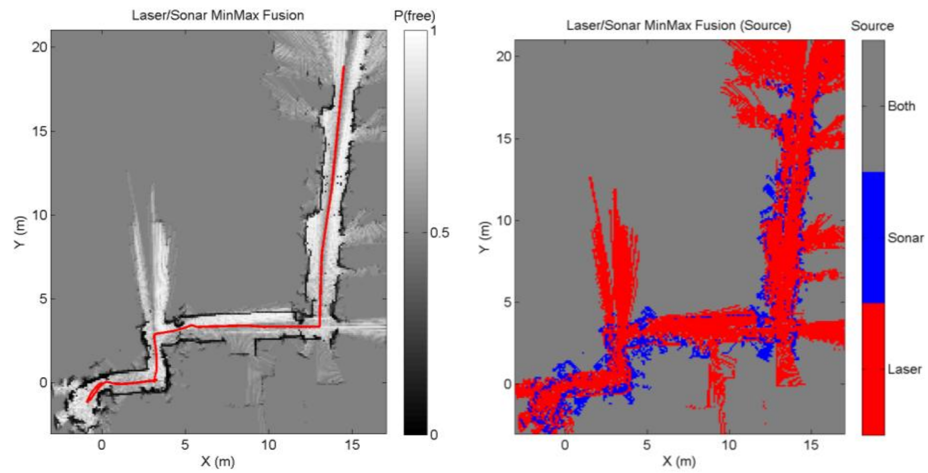

Figure 5: Occupancy grid map generated from multiple sensors using the MinMax fusion algorithm.

It should be noted that the model parameters (such as sensor evidence weights and sampling rates) likely affect how well each sensor – and therefore the fusion of sensors – can predict the binary state of the occupancy grid cells. Therefore, the presentation of the MinMax fusion algorithm is not meant to be stated as superior in general; rather, it is presented for future study in multiple sensor indoor mapping as one of several algorithm options for sensor fusion.

Conclusions

This study demonstrated that the indoor environment was successfully mapped using an occupancy grid, where each cell in the grid was modeled as a binary random variable representing whether the cell was free or occupied. The probability estimates (grid cells) were updated as the algorithm processed robot evidence (odometry, laser, and sonar) in real-time. The predicted map of the indoor environment was shown to be similar to the qualitative ground truth map, if odometry errors are neglected. The MinMax fusion algorithm was shown to slightly improve the probability estimates of the sensor fusion map as compared to the map generated by the laser data alone. However, this algorithm may be sensitive to the object types within the indoor environment and the model and sensor parameters, so further study is recommended.

Future Work

The current study explores the nature of mapping an indoor environment using multiple sensors, and there are several paths forward of future work. To extend the work to the entirety of the indoor environment, it is necessary to correct for odometry errors. It may be possible to join small submaps together in a technique such as Linear SLAM that avoids issues with odometry errors [6]. The generality of the MinMax sensor fusion algorithm is also intriguing, and it would be beneficial to understand how sensitive this fusion algorithm is to sensor evidence weights, indoor obstacles, and other parameters of the map and sensor models. Lastly, it would be intriguing to cross-reference the mapping method implemented in this study with open-source methods, such as those provided by the CARMEN toolbox, as a means of cross-validation [7].

References

[1] A. Howard, N. Roy, The Robotics Data Set Repository (Radish), 2003. http://radish.sourceforge.net/.

[2] S. Thrun, W. Burgard, and D. Fox. *Probabilistic Robotics*, MIT Press, 2005.

[3] “Pioneer 2 Mobile Robot – Operation Manual,” January 1999.

[4] C. Tarin Sauer, H. Brugger, E. P. Hofer, B. Tibken, “Odometry Error Correction by Sensor Fusion for Autonomous Mobile Robot Navigation,” *IEEE Instrumentation and Measurement Technology Conference*, May 21-23, 2001.

[5] J. Borenstein, L. Feng, “UMBmark: A Benchmark Test for Measuring Odometry Errors in Mobile Robots,” SPIE Conference on Mobile Robots, 1995.

[6] L. Zhao, S. Huang, G. Dissanayake, “Linear SLAM: A Linear Solution to the Feature-based and Pose Graph SLAM based on Submap Joining,” *Proceedings of the 2013 IEEE/RSJ International Conference on Intelligent Robots and Systems*, November 3-7, 2013.

[7] M. Montemerlo, N. Roy, S. Thrun, “Perspectives on Standardization in Mobile Robot Programming: The Carnegie Mellon Navigation (CARMEN) Toolkit,” *Proceedings of the 2003 IEEE/RSJ International Conference on Intelligent Robots and Systems*, October 27-31, 2003.